

Inhibition mechanism and corrosion protection of mild steel in HCl using coumarin derivative: Gravimetical and theoretical analysis

H.M. Luaibi,¹ N. Betti,² S.S. Al-Taweel,³ T.S. Gaaz⁴ 
and A.A. Alamiery^{5,6} 

¹Al-Karkh University of Science, College of Energy and Environmental Sciences,
Department of Renewable Energy, Baghdad-10081, Iraq

²Materials Engineering Department, University of Technology-Iraq, Baghdad 10/001, Iraq

³Al-Karkh University of Science, College of Science, Department of forensic Science,
Baghdad-10081, Iraq

⁴Air Conditioning and Refrigeration Techniques Engineering Department, College
of Engineering and Technologies, Al-Mustaqbal University, Babylon 51001, Iraq

⁵University of Technology, Baghdad P.O. Box 10001, Iraq

⁶University Kebangsaan Malaysia, Bangi P.O. Box 43000, Selangor, Malaysia

*E-mail: dr.ahmed1975@gmail.com

Abstract

This research investigates the potential of 2-((2-oxo-2H-chromen-7-yl)oxy)acetic acid (CAE) to inhibit mild steel corrosion in 1 M hydrochloric acid using gravimetical methods and scanning electron microscopy (SEM). The study explores the adsorption and inhibition mechanisms through weight loss analysis and density functional theory (DFT) calculations. The inhibitor exhibited a maximum efficacy of 87.5% at a concentration of 0.5 mM after a 10-hour immersion period at 303 K. Experiments conducted at different immersion times (5, 10, 24, and 48 hours) revealed 10 hours to be the most effective duration for the chosen inhibitor concentrations (0.1–1.0 mM) at 303 K. Inhibition efficiency increased proportionally with rising inhibitor concentration and remained stable beyond 10 hours up to 48 hours. The influence of temperature on the inhibition process was studied for varying inhibitor concentrations. Here again, 10 hours emerged as the optimal immersion time. The Langmuir adsorption isotherm model was successfully applied to understand the inhibitor's adsorption behavior on the mild steel surface. The variation in activation energy demonstrated that particular binding incidents existed between the inhibitor compounds and the cast mild steel surface. The DFT calculations made this interaction more vivid by providing more insight into them. Analysis found a slight difference in energy between HOMO and LUMO which proved the inhibitor effectiveness. The relevant data of the experiments and calculations show a good correspondence, which proves the efficacy of CAE as a corrosion inhibitor for mild steel in HCl environment.

Received: March 15, 2024. Published: June 5, 2024

doi: [10.17675/2305-6894-2024-13-2-23](https://doi.org/10.17675/2305-6894-2024-13-2-23)

Keywords: steel, HCl, coumarins, corrosion inhibition, green inhibitor.

1. Introduction

It is known that metals are susceptible to corrosion when exposed to acidic atmospheres directly in a solution of hydrochloric acid, which is a compound commonly used for industrial purposes [1, 2]. Consequently, this effect triggers electrochemical reactions, and the end result is that the metal will crumble and collapse. Chloride ions form hydrochloric acid solutions that facilitate rust by corroding the oxide layer on the surface of the object, which is highly corrosive. Corrosion is a cost-consuming phenomenon in itself. This results in some direct costs related to items such as material replacement, maintenance and repair. On the other hand, there are other expenses, such as production delays and reduced operating efficiency, which result from unforeseen conditions and downtime [6, 7]. Global spending on corrosion can reach billions annually and the impact has been most significant for industries that rely heavily on metal facilities, such as manufacturing, aviation, and oil and gas [8, 9]. The use of corrosion inhibitors constitutes the first approach aimed at reducing the harmful consequences of corrosion [10, 11]. Over time, phosphates, chromium, *etc.* were used as dandruff inhibitors. While the environmental impact of electric vehicles on the environment continues to be a concern which has led to a search for more environmentally friendly options, during this time, legal issues still remain. Natural corrosion inhibitors that are mainly based on organic materials come from areas where organic materials have already proven effective against corrosion. Coumarins, a family of aromatic compounds of which plants serve as a source, are said to possess multiple beneficial corrosion-inhibiting properties [16–21]. The flexible structure of the proposed design will include the necessary changes that will improve its efficiency. Furthermore, they are less aggressive towards the environment since their biodegradability and inherent non-toxicity make them cleaner than their conventional retardant counterparts. Scientists are investigating the ability to provide N, O, S and P heteroatoms in organic compounds to discover more corrosion inhibitors. These components can be important in forming the protective layer over the metal surface, which plays an essential role in preventing corrosion mechanisms. DFT is responsible for the tremendous success in the field of theoretical studies of corrosion, due to its unique ability to detect not only actually existing corrosion but also explain the origin of a particular type of corrosion. Thus, studying corrosion mechanisms at the molecular level with an emphasis on the interaction between metal surfaces and their surroundings is of fundamental importance for the invention of effective corrosion inhibitors [27]. DFT is just one of the very useful tools to study inhibitor adsorption on metal surfaces. It assumes a theoretical model to predict the electronic behavior and properties of solid materials [28]. Thus, by reproducing the behavior of inhibitory molecules upon contact with metal atoms, DFT will provide precise thermodynamics and kinetics of inhibitor adsorption, providing significant assistance in identifying factors that reduce inhibitor efficiency. This approach was one of the determinants of the optimal properties of chemical inhibitor molecules to facilitate fixation on the metal surface in order to prevent the corrosion process. DFT studies predict the nature of inhibitor adsorption by digitizing the electronic structure and charge

distribution of complexes formed between the inhibitor and metals via computational simulations. This knowledge allows the creation of new intellectually designed inhibitors with better drug efficiency [30]. Furthermore, DFT calculations can shed light on the precise role of certain heteroatoms or functional groups within inhibitor molecules with respect to adsorption as well as nucleation and dissolution of aggressive elements. For example, besides O, N, S, and P, such interactions between inhibitor molecules and metals come in the form of adsorption that prevents oxidation of the metal. Also, DFT investigations will provide examples of the mechanisms of corrosion inhibitors by considering features of the reaction pathways and energetics that occur in the presence of the inhibitor. The DFT model can explain how inhibitors change the reactivity of metal atoms through their kinetic and thermodynamic interactions, hindering the formation of corrosion products [31]. More clearly, the goal is to better understand the inhibition process, and DFT provides essential knowledge of all available molecular level details. This research investigates the potential of a new coumarin derivative, CAE (Figure 1), as a corrosion inhibitor for mild steel in a 1 M HCl solution. Our aim is to analyze and understand the inhibitory properties of CAE, thereby contributing to the development of efficient and sustainable corrosion inhibition strategies. This study aims to elucidate the fundamental mechanisms by which CAE inhibits corrosion.

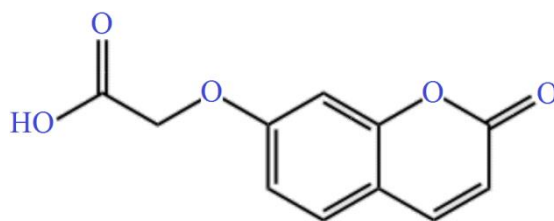


Figure 1. The chemical structure of CAE.

2. Experimental Procedure

2.1. Material preparation

The corrosion inhibitor utilized in this study can indeed be obtained commercially from Sigma-Aldrich. Additionally, the compound can also be readily synthesized in the laboratory using the method outlined in reference [32]. Mild steel samples with the following composition (wt.%) were used: 0.21 C, 0.38 Si, 0.05 Mn, 0.09 P, 0.01 Al, and the balance Fe. The samples ($4.5 \times 1 \times 0.5$ cm) were prepared according to ASTM G1-03 guidelines. To achieve a smooth and reflective surface, the samples were mechanically polished with fine-grit sandpaper, eliminating any surface imperfections. Following cleaning with acetone and deionized water, the samples were air-dried to minimize oxide layer formation. Finally, surface profiling using profilometry ensured smoothness and consistency.

2.2. Test solution preparation

A 1 M hydrochloric acid (HCl) solution was prepared by diluting analytical grade HCl in distilled water. CAE concentrations ranging from 0.1 to 1 mM were employed in an electrolyte solution with a total volume of 100 mL. A blank solution containing only 1 M HCl served as a comparison. Different CAE concentrations were added to the 1 M HCl solution to assess their corrosion inhibition effectiveness. Thorough mixing ensured even distribution of the inhibitor within the acidic medium [33, 34].

2.3. Weight loss test

This method, valued for its simplicity, was used to measure corrosion rates. Cleaned, dried, and weighed samples were immersed in 100 mL of HCl solution with varying CAE concentrations at room temperature. After specific durations (2, 5, 10, 24, and 48 hours), samples were removed, cleaned, and reweighed. Each sample was weighed three times before and after immersion for accuracy [35, 36]. The symbol ΔW (Equation 1) represents the average weight loss in milligrams (mg). The variable W_0 represents the starting weight of the specimen without inhibitors, while W_i represents the weight of the specimen with inhibitor.

$$\Delta W = W_0 - W_i \quad (1)$$

Corrosion rate (C_R), inhibition efficiency (%*IE*), and surface coverage (θ) were calculated using relevant formulas 2–4 [37–39].

$$C_R \text{ (mpy)} = \frac{534 \cdot \Delta W}{\rho a t} \quad (2)$$

$$\% IE = \frac{C_{R_0} - C_R}{C_{R_0}} \cdot 100 \quad (3)$$

$$\theta = \frac{C_{R_0} - C_R}{C_{R_0}} \quad (4)$$

Three replicates were used for each test [40–43].

2.4. Density functional theory (DFT) calculations

The interaction between the inhibitor and the metal surface was investigated through density functional theory (DFT) simulations. Calculations were performed with the Gaussian 09 software package employing the B3LYP functional in the gas phase, along with the 6-31G++(d,p) basis set [44, 45]. It turned out crucial to identify the electric features of the inhibitor and how it reacts to the metal surface during the calculation process. The experiment proposed *I* (ionization potential) and *E* (electron affinity), which are two fundamental characteristics that can irradiate Koopmans' theory using the highest occupied

molecular orbital (E_{HOMO}) and the lowest unoccupied molecular orbital (E_{LUMO}), respectively. For example, some of the most important chemical traits like electronegativity and degree of hardness and softness were also determined.

Through the implementation of these formulae one could obtain qualitative concept about the role of the inhibitor and its interaction with the surface of the metal. The subsequent equations were employed for the computation of I and A : The subsequent equations were employed for the computation of I and A :

$$I = -E_{\text{HOMO}} \quad (5)$$

$$A = -E_{\text{LUMO}} \quad (6)$$

Lastly, important chemical features like the electronegativity (χ), the hardness (η), and the softness (σ) were determined precisely with the use of the equations given in reference [46].

$$\chi = \frac{I + A}{2} \quad (7)$$

$$\eta = \frac{I - A}{2} \quad (8)$$

$$\sigma = \frac{1}{\eta} \quad (9)$$

This way, the more information was received about what its electrical properties are, as well as how it likes to interact with the metal of the surface. That is the data from which we can learn if the inhibitor is very strong or very weak. The real story in this environment is about the differentiation of electronegativity (the electron pull tendency) of the inhibitor and that of the metal (iron is the case). A custom equation was the Equation 2 and the specific features of iron were considered in the process of calculating the equation, thus deducing ΔN (Equation 10) [46]. With this value we can measure the penetration capability of the inhibitor into the metal surface and thereby the formation of the protective layer on the metal.

$$\Delta N = \frac{\chi_{\text{Fe}} - \chi_{\text{inh}}}{2\eta_{\text{Fe}} + 2\eta_{\text{inh}}} \quad (10)$$

$$\Delta N = \frac{7 - \chi_{\text{inh}}}{2\eta_{\text{inh}}} \quad (11)$$

2.5. Adsorption isotherm investigations

Adsorption isotherm was the model of choice to explain the binding process between inhibitor and metal surface. These models help us understand how much of the metal surface the inhibitor covers (coverage) and how this coverage changes depending on the surrounding environment (the corrosive solution in this case). One model, the Frumkin isotherm, takes

into account how closely packed the inhibitor molecules are on the surface. This closeness can affect how effectively the inhibitor forms a protective layer. The mathematical representation of it is denoted as [47]:

$$n = \frac{RT}{\mu} \ln(K_f) + \beta \frac{n^2}{2RT} \quad (12)$$

where, n is the surface coverage of the inhibitor, K_f represents the Frumkin adsorption equilibrium constant, β donates for the lateral interaction coefficient, μ signifies the chemical potential, R is the constant of ideal gas, and T represents for temperature in Kelvin.

Another model, the Temkin isotherm, considers the fact that as more inhibitor molecules attach to the surface, it becomes slightly less attractive for additional molecules to join. This reflects the decreasing interaction between the inhibitor and the metal as the surface gets covered. Its formula is given by:

$$A = RT \ln b + \frac{RT}{b} \theta \quad (13)$$

In this equation, b represents the Temkin isotherm constant associated with the heat of adsorption, A denotes the Temkin isotherm constant related to the equilibrium binding constant, and θ stands for the fraction of occupied surface sites.

Finally, the Langmuir isotherm assumes a scenario where the inhibitor forms a single, uniform layer on the metal surface. This is a commonly used model for understanding how corrosion inhibitors work. It's expressed as:

$$\theta = \frac{K_{\text{ads}} \cdot C_{\text{inh}}}{1 + K_{\text{ads}} \cdot C_{\text{inh}}} \quad (14)$$

Here, K_{ads} is the Langmuir constant, C_{inh} denotes the concentration of tested inhibitor, and θ represents the surface coverage.

In addition to these theoretical models, we conducted experiments to measure the actual weight loss of the metal under different inhibitor concentrations. This real-world data allowed us to compare it with the predictions from the models, confirming our understanding of how the inhibitor behaves on the metal surface [48].

3. Results and Discussion

3.1. Weight loss measurements

Figure 2 shows how effectively CAE acts as a corrosion inhibitor for mild steel in a strong acid solution (1 M HCl) after 5 hours of immersion. It has been assessed by the way, in which we weighed the metal to know the exact loss. If the level of CAE intensified, its corrosion rate would be lowered. Carrying out the test without any corrosion inhibitor (0 mM) brought about a corrosion rate as high as 521 mpy. On the other hand, a high CEA concentration may result in pitting corrosion which will occur at very low rates of ~49 mpy

and 38 mpy. This from the fact that highest corrosion resistance was achieved when nitriding was performed and CAE was used as surface finish implies that as a protective layer CAE can successfully protect the metal from severe acidic environment [49, 50]. With addition of the concentration level, CAE can significantly reduce a corrosion amplitude. At a low dose (0.1 mM), the CAE, as measured with the inhibition of about 44.8%, is at low level. While at higher concentrations (0.5 mM and 1 mM) superiority in the inhibition effect can be seen even higher degrees like 87.5% and 91.2% respectively. This demonstrates a considerable decrease in corrosion, indicating the superiority of CAE as an inhibitor. Recognize the grammar structures such as modals, pronouns, and verb tenses that are commonly used in this specific language. Achieve fluency in the key sentence patterns of both spoken and written communication within the context of the target language. In the last instance, it can be concluded that the workability of CAE as an anti-corrosion material for mild steel in acidic conditions is very capable. The observation of a marked decline in corrosion magnitude and acceleration of the inhibition efficiency with the increasing CAE concentration implies a broad area application of the inhibitor for different industrial utilizations.

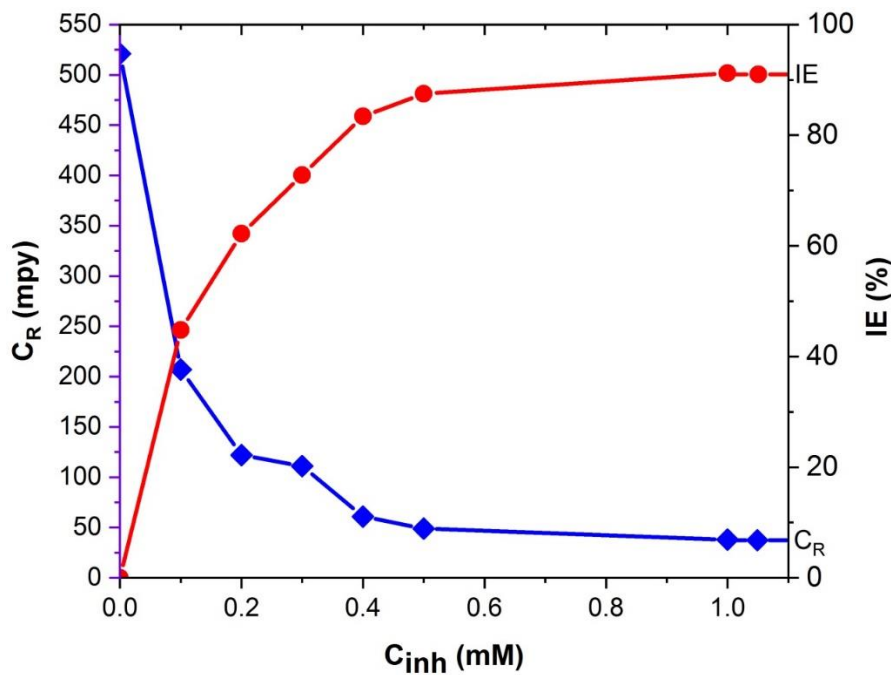


Figure 2. Effect of inhibitor concentration on corrosion rate and inhibition efficiency of CAE in 1 M HCl solution.

3.2. Effect of immersion time periods

Figure 3 shows the effects of exposure duration on filled tube immersion time on CAE corrosion inhibition capacity. Process monitoring was carried out by utilizing weight loss measurements for measuring the influence of CAE concentration on corrosion rate. Incredibly, corrosion rate went down with exposure time raise in acidic surrounding for each

of three CAE concentrations. For instance, there is a discrepancy between corrosion rates (276 mpy after 0.1 mM exposure for 1 hour and 173 mpy with the same exposure for 48 hours). This holds true not just for the lower CAE levels [52, 53] but it also for the higher concentrations. This implies that the French twist performed over extended time frames becomes more successful in the metal protection process. Inhibition efficiency, like corrosion rate, is better as the exposure time duration expands and concentration increases. At a low CAE concentration (0.1 mM), the initial inhibition is moderate (29.6%) but increases to 61% after 48 hours. At a higher concentration (1 mM), the initial inhibition is already strong (83%) and further improves to 94% after 48 hours. This indicates that CAE's effectiveness increases the longer the metal is exposed to the acid, with higher concentrations offering even greater protection over time [54]. Overall, the results show that both the duration of exposure and the amount of CAE used are crucial factors in its effectiveness as a corrosion inhibitor. CAE's ability to slow down corrosion and improve its protective effect over time suggests its potential for applications requiring long-term protection against acidic environments.

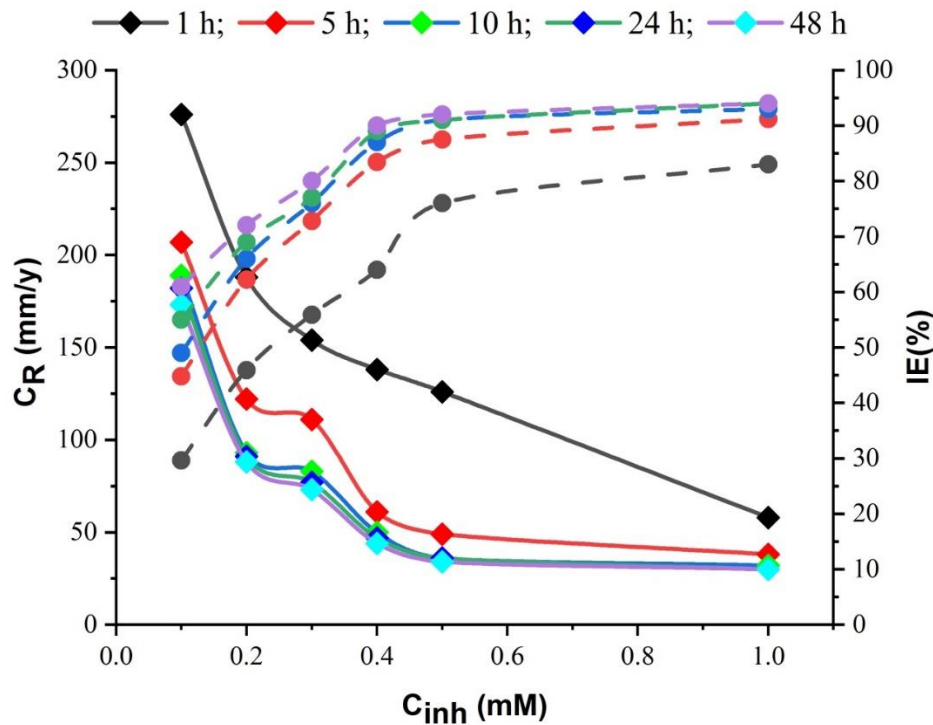


Figure 3. Effect of immersion time on corrosion rate and inhibition efficiency of CAE in 1 M HCl solution.

3.3. Effect of temperature

Figure 4 explores the influence of temperature on the corrosion protection efficacy of CAE for mild steel in a strong acidic environment (1 M HCl). Weight loss measurements were employed to quantify this effect. The relationship between temperature and corrosion rate is complex and will be further discussed. At lower temperatures (303 K), higher CAE

concentrations lead to slower corrosion [55]. For example, with a low CAE concentration (0.1 mM), the corrosion rate is higher at a higher temperature (141 mpy at 333 K compared to 207 mpy at 303 K). This suggests CAE performs better in cooler environments. Similar to the corrosion rate, CAE's ability to prevent corrosion (inhibition efficiency) is also affected by temperature. Lower temperatures generally favor higher inhibition. At a low CAE concentration (0.1 mM) and lower temperature (303 K), the initial inhibition is moderate (44.8%). Interestingly, at the same concentration but a higher temperature (333 K), the initial inhibition increases (91.2%). However, at even higher temperatures, further increases in CAE concentration might not significantly improve inhibition. This indicates that while CAE remains effective at various temperatures, extremely hot environments can slightly reduce its effectiveness [56]. Overall, the results highlight that temperature plays a role in CAE's performance as a corrosion inhibitor. Cooler temperatures and higher CAE concentrations generally lead to better protection. These findings emphasize the importance of considering temperature variations when selecting corrosion inhibitors for industrial applications [57, 58].

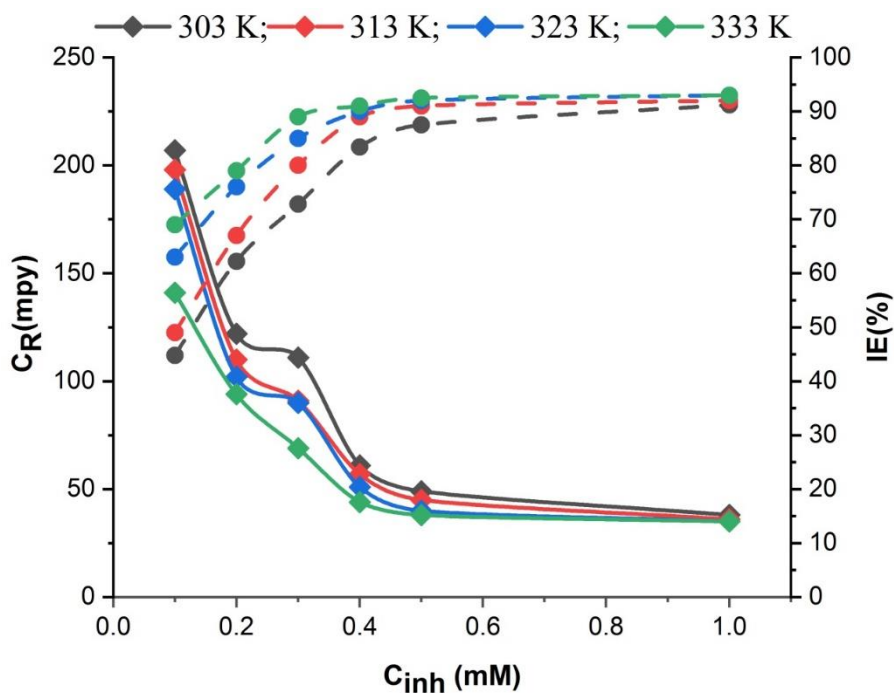


Figure 4. Effect of temperature on corrosion rate and inhibition efficiency of CAE in 1 M HCl solution.

3.4. Adsorption isotherm

The way an inhibitor interacts with the metal surface can be analyzed through a special kind of graph called an “adsorption isotherm”. This graph helps us understand how much of the metal surface the inhibitor covers (coverage) and how this changes with the amount of inhibitor used (concentration). A higher starting point (intercept) on the graph generally indicates a stronger bond between the inhibitor and the metal. This translates to a larger area

of the metal surface being covered by the inhibitor [59]. The slope of the graph reflects the change in inhibitor coverage with increasing inhibitor concentration. A steeper slope indicates that adding more inhibitor has a larger impact on the coverage, while a flatter slope suggests smaller changes [60]. Looking at Figure 5, the Langmuir isotherm appears to best represent how the inhibitor molecules interact with the mild steel surface. This is because the data points closely follow a straight line, signifying a strong correlation between the amount of inhibitor used and the resulting coverage. The Langmuir adsorption constant (K_{ads}) was determined according to Equation 14, derived from Equation 15 [61]:

$$K_{\text{ads}} = \frac{\theta}{C_{\text{inh}}(1-\theta)} \quad (15)$$

Another important parameter is the standard free energy of adsorption, which tells us if adsorption happens spontaneously. A negative value suggests that adsorption is favorable and happens spontaneously. The Gibbs free energy of adsorption (ΔG_{ads}) can be calculated based on Equation 16, [62]:

$$\Delta G_{\text{ads}}^0 = RT \ln(55.5) \quad (16)$$

where: R is the gas constant (8.314 J/mol·K), T is the temperature in Kelvin (assumed to be constant), and 55.5 is the concentration of water (in mol/L).

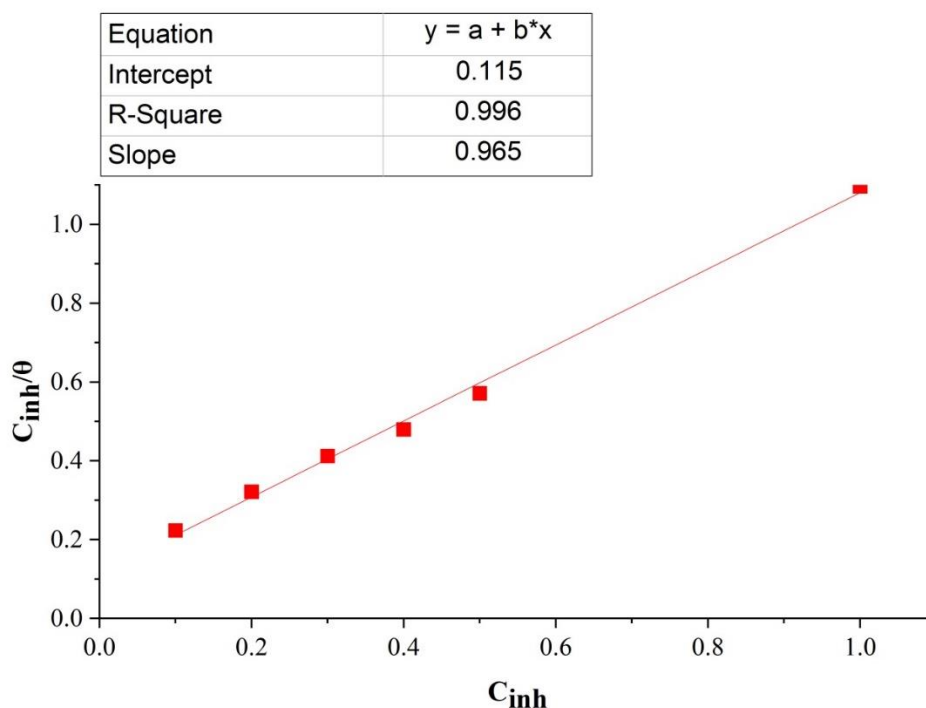


Figure 5. Langmuir adsorption isotherm analysis of CAE on mild steel surface in 1 M HCl solution.

Our calculations show a value of -9.887 kJ/mol, indicating that CAE readily adheres to the mild steel surface. This spontaneous adsorption is a crucial factor for effective corrosion inhibition. In simpler terms, CAE sticks well to the metal, forming a protective layer that shields it from the corrosive environment. This “sticking” is essential because it prevents the corrosive agents from reaching the metal surface and causing damage. The type of bond formed between CAE and the metal surface is crucial. Scientists use a special graph called the “Langmuir adsorption isotherm” to analyze this interaction. This graph suggests that CAE forms physical adsorption. The specific pattern observed in the Langmuir plot indicates that CAE forms a single layer on the metal surface, further strengthening the protection [63].

The calculations indicate a value of -9.887 kJ/mol, which suggests a strong attraction between the inhibitor and the mild steel surface. The calculated value falls within the range characteristic of physical adsorption [64].

3.5. Thermodynamic analysis of CAE in 1.0 M HCl solution

The standard adsorption enthalpy (ΔH^0) for the inhibition process can be calculated according to Van't Hoff equation (Equation 17):

$$\frac{d \ln K}{dT} = \frac{\Delta H^0}{RT} \quad (17)$$

By rearranging Equation 17, we obtain Equation 18 [63, 64]:

$$\ln K = \frac{-\Delta H^0}{RT} + A \quad (18)$$

where A is the integral constant.

The linear correlation coefficient (R^2) for CAE, as shown in Figure 6, is 0.998. From the slope of the straight line of $\ln K$ versus T , the values of ΔH^0 are calculated and summarized in Table 1.

Table 1. Thermodynamic parameters for CAE in 1.0 M HCl.

Temperature (°C)	ΔG^0 (kJ/mol)	ΔH^0 (kJ·mol ⁻¹)	ΔS^0 (J·mol ⁻¹ ·K ⁻¹)
303	-9.887	37.46	266.87
313	-21.63	41.26	225.59
323	-23.26	41.27	224.60
333	-24.55	42.84	218.33

Based on Equation 14 and obtained K values, the free energy of adsorption (ΔG^0) is calculated. The standard thermodynamic parameters are then compiled in Table 2. The positive values of ΔH^0 indicate that the adsorption of the inhibitor is endothermic.

Interestingly, an increase in temperature correlates with an increase in inhibition efficiency, suggesting a potential involvement of the inhibitor in a chemical adsorption process at higher temperatures. Moreover, the ΔG^0 value provides additional insights. When ΔG^0 is larger than -20 kJ/mol, it signifies electrostatic interaction between the charged inhibitor and the charged steel, indicating physical adsorption. Between -21 kJ/mol and -25 kJ/mol (at 313 K to 333 K), the adsorption involves the transfer of the charged organic inhibitor onto the steel surface, resulting in the formation of a coordinated bond (chemical adsorption) along with physical bonds. Essentially, there exists no clear boundary between physical and chemical adsorption, as physical adsorption can be considered the initial stage of chemical adsorption. Furthermore, the negative ΔG^0 values at the same temperature indicate strong adsorption of CAE on the steel surface. The positive sign of ΔS^0 indicates an increase in entropy, suggesting enhanced chaos between reactant molecules on the metal electrode surface. This increase in chaos serves as an important driving force for inhibitor molecules to adsorb onto the metal surface [63, 64].

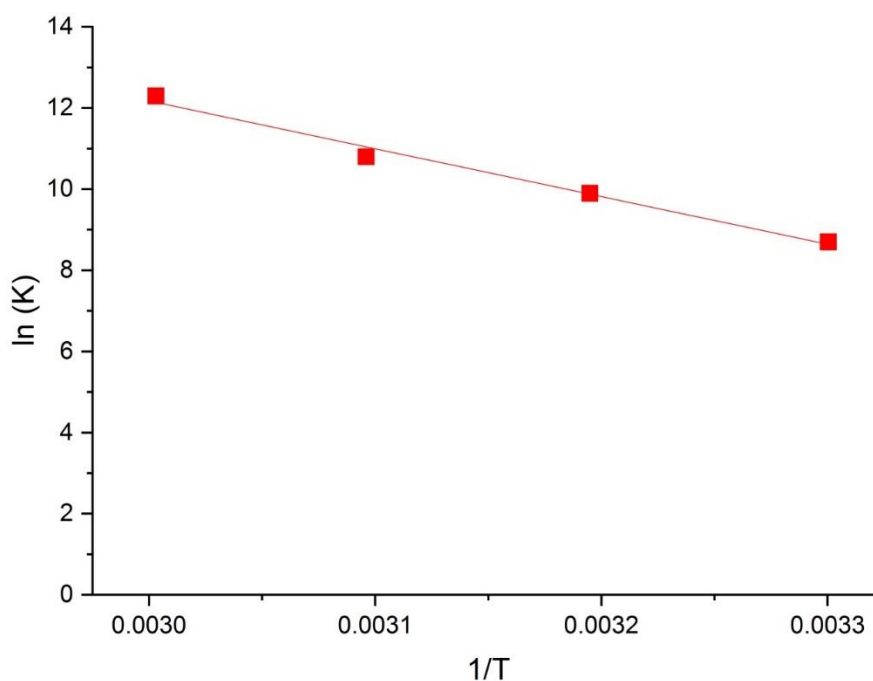


Figure 6. Straight line of $\ln K$ versus $1/T$.

3.6. SEM

In order to observe the surface morphology of the metallic sample in the absence and presence of tested inhibitor, the mild steel coupons were analyzed by scanning electron microscopy (SEM) employing a scanning electron microscopy, type TM1000 Hitachi Tabletop Microscope at $2000\times$ magnification was used. Before carrying out these analyses, the metallic samples were polished until reaching a mirror finishing and were submitted to immersion for 5 h in the absence and presence of 0.5 mM of tested inhibitor at 303 K. Figure 7 shows the surface analysis of the steel sample after its exposure to 1 M HCl in the

absence and presence of tested inhibitor at 303 K for 5 h by SEM. Figure 7a displays the blank micrograph with evident surface damage and heterogeneous morphology caused by Cl^- and H_3O^+ ions, which are characteristic of the corrosive medium and by the temperature effect. In the presence of tested inhibitor at 0.5 mM (Figure 7b), a less damaged and more homogeneous morphology is observed; even some surface fractions spared by the corrosive attack can be seen, which reveals higher corrosion resistance originated by the adsorption of a CI protecting film.

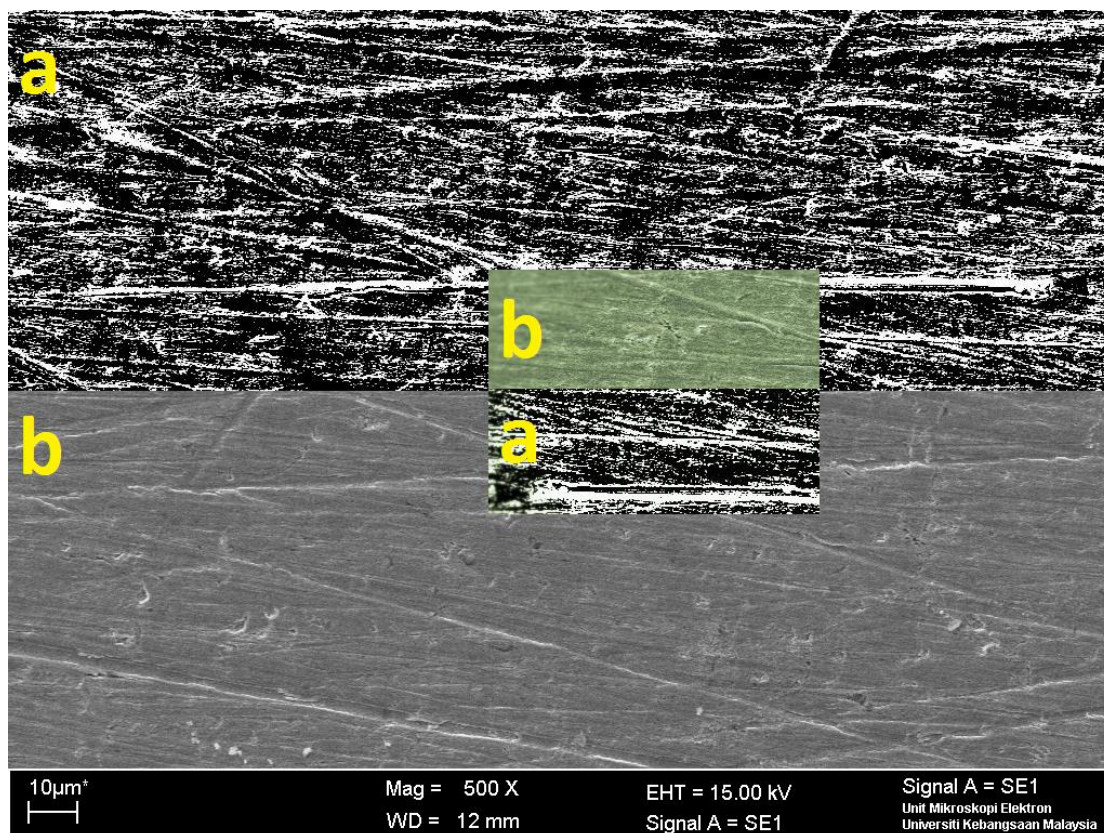


Figure 7. SEM micrographs of mild steel exposed to 1 M HCl at 300 K in the presence of: (a) 0 mM CAE, and (b) 0.5 mM of CAE.

3.7. DFT calculations

Imagine a powerful computer program that can act like a virtual laboratory for studying the building blocks of our world: molecules and materials. This is exactly what density functional theory (DFT) offers. DFT is a computational tool used in quantum mechanics, a branch of physics that deals with the very small. DFT allows us to predetermine the qualities of molecules and materials by using experiments without spending lot [65]. DFT helps us understand the arrangement and behavior of electrons within molecules and materials. This includes determining their energy levels, how easily they can be removed (ionization energy), and their attraction to other atoms (electronic affinity). DFT has become a cornerstone in chemistry and material research. Scientists use it to predict how molecules

and materials will behave under various conditions, including their susceptibility to corrosion (rusting). By simulating the interaction between inhibitor molecules and metal surfaces, DFT helps researchers develop more effective ways to prevent corrosion [66, 67]. This section explores the properties of the inhibitor molecule through various calculations. Imagine the electrons in a molecule occupy different “energy levels”. The gap between the highest occupied level (HOMO) and the lowest unoccupied level (LUMO) is called the energy gap. A larger gap (7.723 eV in this case) signifies that more energy is needed to move an electron from its current position (Table 2). Ionization energy refers to the energy required to remove an electron from the molecule entirely. A higher value (12.088 eV) indicates the molecule holds its electrons tightly. Electron affinity is the opposite of ionization energy. It represents the energy released when the molecule gains an electron. A lower value (4.365 eV) suggests the molecule has some capacity to accept additional electrons. Electronegativity reflects how strongly an atom or molecule attracts electrons. It’s calculated as an average of ionization energy and electron affinity (8.227 eV in this case). Hardness and softness terms describe how easily the molecule’s electron distribution can be altered. A higher global hardness (3.862 eV) indicates resistance to such changes. Conversely, softness (0.259) reflects the ease with which the molecule can share electrons. Electron transfer calculation (−0.3217) suggests that the inhibitor molecule tends to donate some electrons to the metal surface. This electron transfer contributes to the formation of a protective layer on the metal [68, 69].

Table 2. Electronic parameters of CAE calculated via density functional theory (DFT).

Parameter	Value
Energy gap (ΔE)	7.723 eV
Ionization energy (I)	12.088 eV
Electronic affinity (A)	4.365 eV
Electronegativity (χ)	8.227 eV
Global hardness (η)	3.8615 eV
Softness (σ)	0.259 eV ⁻¹
Fraction of transferred electrons (ΔN)	−0.3217

Figure 8a shows the 3D structure of the inhibitor molecule. Figures 8b and 8c provide additional insights into how electrons are distributed within the molecule. Figure 8b depicts the delocalization of the highest occupied molecular orbital (HOMO) electrons across the entire molecule. This even distribution, called delocalization, signifies stability and lower reactivity. In the context of corrosion inhibition, a stable and evenly distributed electron cloud suggests a higher potential for the molecule to donate electrons. This explaining fact that the molecule can transfer its electrons to the metal makes this molecule develop strong bonds with the metal surface which would enable the molecule to act as an anti-corrosion

agent. The relationship between the Figures 8b and 8c reveals that electrons are distributed within the inhibitor in the molecular level. It is quite significant to understand the function of such a substance, whether it does prevent the corrosion or not. It is zone 8b where the molecule is easily capable to transfer and share electrons (HOMO). This way of classification is also an indicator of the relaxation and indicates that this molecule is more likely to give electrons donation. In corrosion avoiding, this skills of sharing electrons are very imperative to make the surface of metal strong. Figure 8c gives us the information about the localization of the parts (aromatic and pyrone rings) where the molecule lifts the electrons (LUMO). It means these regions can contain these elements or fix them to the metal.

Together, Figures 8a, 8b, and 8c suggest that the inhibitor molecule possesses properties that make it effective in preventing corrosion:

- Electron donation: The configuration of the molecule eases the process of exchanging electrons, thus creating a strong link with metal atoms surface.
- Targeted interaction: Certain areas within the molecule are believed to be more able to accept electrons to form a bond with that of the metal, hence the complementary property that facilitates corrosion protection.

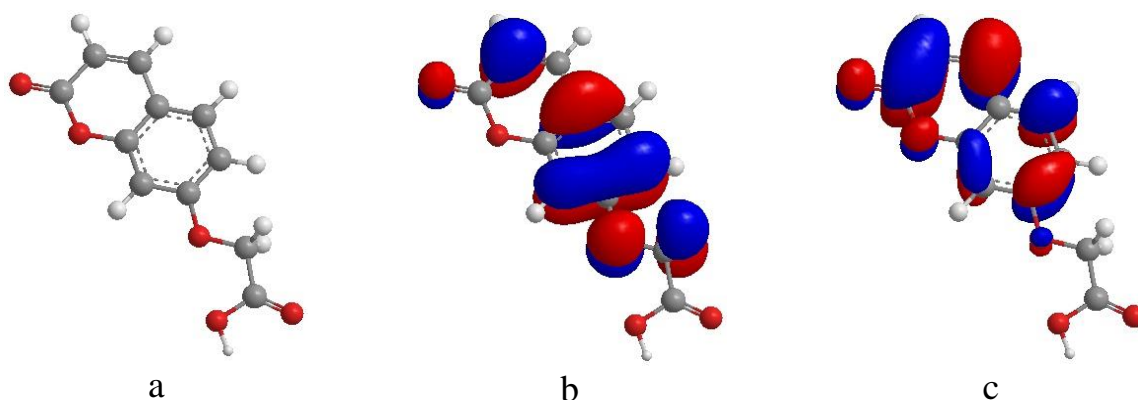


Figure 8. The (a) optimized structure, (b) E_{HOMO} , and (c) E_{LUMO} of inhibitor molecules.

3.8. Comparison of coumarins as corrosion inhibitors

Coumarins, a class of organic compounds containing the benzopyrone structure, have gained significant attention as corrosion inhibitors due to their favorable adsorption characteristics and chemical properties. In this section, we compare the performance of various coumarin derivatives as corrosion inhibitors with our studied inhibitor (Table 3), 2-((2-oxo-2*H*-chromen-7-yl)oxy)acetic acid (CAE), against mild steel in acidic environments. A comparison of various coumarin-based corrosion inhibitors highlights their inhibition efficiency, advantages, and limitations, providing insights into their potential applications in corrosion control. PMBH demonstrates an impressive inhibition efficiency of 98.8%, coupled with eco-friendliness. However, its synthesis process is costly and challenging [71]. (2-(7-hydroxy-2-oxo-2*H*-chromen-4-yl)acetyl)- β -alanine with an inhibition efficiency of 71.74%, this compound offers eco-friendly corrosion protection. Nonetheless, its synthesis

is expensive and complex [2]. (2-(7-Hydroxy-2-oxo-2*H*-chromen-4-yl)acetyl)- β -alanine methyl ester, (2-(7-hydroxy-2-oxo-2*H*-chromen-4-yl)acetyl)- β -alaninehydrazide, and (2-(7-hydroxy-2-oxo-2*H*-chromen-4-yl)acetyl)- β -alanylglycine exhibit inhibition efficiencies ranging from 40.04% to 53.04%, providing eco-friendly corrosion protection. However, they show relatively lower efficiency compared to other inhibitors [72]. EFCI with a high inhibition efficiency of 94.7%, EFCI offers eco-friendly corrosion protection. However, its efficiency decreases with temperature [73]. BTMC and BTC demonstrate inhibition efficiencies of 93.5% and 92.1%, respectively, and are known for effective adsorption and suitability for acidic environments. However, they exhibit lower efficiency at high concentrations and specificity towards certain acids [74, 75]. 8-Piperazine-1-ylmethyl-umbelliferone provides eco-friendly corrosion protection with an efficiency of 93.4%. However, its efficiency decreases with temperature [76]. 4-Hydroxy-3-(phenyldiazenyl)-2*H*-chromen-2-one, 4-hydroxy-3-((4-bromophenyl)diazenyl)-2*H*-chromen-2-one, 4-hydroxy-3-((4-chlorophenyl)diazenyl)-2*H*-chromen-2-one, and 4-hydroxy coumarin offer eco-friendly corrosion protection with inhibition efficiencies ranging from 60.81% to 89%. However, they exhibit lower efficiency at high concentrations and specificity towards certain acids [77, 78].

Table 3. Comparison of coumarins as corrosion inhibitors.

Coumarin	Inhibition Efficiency (<i>IE</i> %)	Advantages	Limitations	Ref.
PMBH	98.8	Ecofriendly, high efficiency	Costly, difficult synthesis	[71]
(2-(7-Hydroxy-2-oxo-2 <i>H</i> -chromen-4-yl)acetyl)- β -alanine	71.74	Ecofriendly	Costly, difficult synthesis	[72]
(2-(7-Hydroxy-2-oxo-2 <i>H</i> -chromen-4-yl)acetyl)- β -alanine methyl ester	47.98	Ecofriendly	Low inhibition efficiency	[72]
(2-(7-Hydroxy-2-oxo-2 <i>H</i> -chromen-4-yl)acetyl)- β -alaninehydrazide	53.04	Ecofriendly	Low inhibition efficiency	[72]
(2-(7-Hydroxy-2-oxo-2 <i>H</i> -chromen-4-yl)acetyl)- β -alanylglycine	40.04	Ecofriendly	Low inhibition efficiency	[72]
EFCI	94.7	Ecofriendly, high efficiency	Decreases with temperature	[73]
BTMC	93.5	Effective adsorption,	Lower efficiency at high concentrations, acid specific	[74]

Coumarin	Inhibition Efficiency (IE%)	Advantages	Limitations	Ref.
		acidic environments		
BTC	92.1	Effective adsorption, acidic environments, potentially biodegradable	Lower efficiency at high concentrations, acid specific	[75]
8-Piperazine-1-ylmethylumbelliferone	93.4	Ecofriendly	Decreases with temperature	[76]
4-Hydroxy-3-(phenyldiazenyl)-2H-chromen-2-one	89	Ecofriendly	Lower efficiency at high concentrations, acid specific	[77]
4-Hydroxy-3-((4-bromophenyl)diazenyl)-2H-chromen-2-one	83	Ecofriendly	Lower efficiency at high concentrations, acid specific	[77]
4-Hydroxy-3-((4-chlorophenyl)diazenyl)-2H-chromen-2-one	86	Ecofriendly	Lower efficiency at high concentrations, acid specific	[77]
4-Hydroxy coumarin	60.81	Ecofriendly	Lower efficiency at high concentrations, acid specific	[78]

3.9. Suggested mechanism

This section explains how the inhibitor molecule interacts with the metal surface to prevent corrosion. The inhibitor molecules attach themselves to the iron atoms on the metal surface. Imagine this attachment as a protective layer that shields the metal from the corrosive environment [79–81]. This attachment involves the inhibitor molecule sharing its electrons with the iron atoms. This protective layer formed by the inhibitor molecules acts as a barrier, preventing the corrosive liquid from directly reaching the metal surface and causing damage. Figure 9 pictorially illustrates the proposed mechanism of how the inhibitor molecule prevents the metal cluster forming [82–85].

The inhibitor molecule's interaction with the metal surface offers additional protection [86–94]. The inhibitor molecule's interaction with the metal surface offers additional protection [86–94]:

- Changing the metal's response: Attaching itself to the metal, the inhibitor modifies the corrosive environment necessity, making it less active and responsive.

- Donating electrons: Inhibition offers up donor electrons to the metal surface which then undergoes reduction. The metal becomes less prone to corrosion at this point. The mentioned electron transfer, apart from that, consolidates the defending the membrane layer.
- Building a physical barrier: Metal surface can indeed induce the reaction between the inhibitor and the cathode of the metal in which a dense, tightly packed layer with small free volume is created. This barrier layer performs the physical role of isolating the stirring and corroding processes and slows them down.

In summary, the inhibitor molecule works by:

- Forming a protective layer: It is bonded to the metal surface, therefore it forms a passivation layer from which the corrosive substance is driven away.
- Reducing metal reactivity: Instead, the alloy resists the formation of new particles and the cracking off of existing ones.
- Providing a physical barrier: This layer of mucus forms a unit which gives barrier and is not accessible to the detrimental substances.

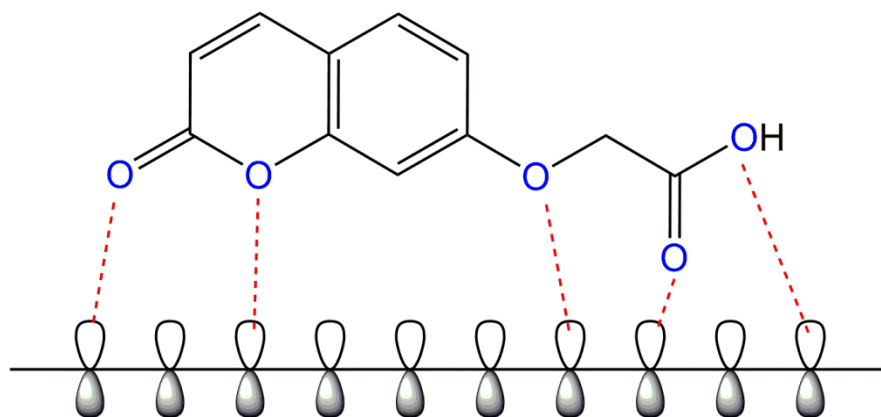


Figure 9. Suggested mechanism.

4. Conclusion

The primary purpose of this research was to look at the prospect of using compound with the formula CAE (2-((2-oxo-2H-chromen-7-yl)oxy)acetic acid) to reduce corrosion of mild steel in a 1 M HCl acid.

Effective corrosion protection:

- Experiments showed that CAE effectively protects the metal, with the best results achieved under specific conditions (high concentration, longer immersion time, and lower temperature).
- Increasing inhibitor concentration and immersion time generally improved protection, while higher temperatures showed a slight decrease in effectiveness.

Understanding the inhibitor:

- Computer simulations (density functional theory) assisted in examining the features of CAE, thus the calculations of its molecular structure and interaction with other compounds enabled deep understanding.

Protective mechanism:

- The theory was developed on the basis that CAE molecules are bonded to the metal surface as an effective protection from the acidic environment. The special micron-thin sheet of uncoating that lays on the surface area of the metals acts as a shielding layer and modify the molecular property the metals to become resistant to various types of damages.

Overall significance:

- This research demonstrates that CAE has promising potential as a practical and eco-friendly corrosion inhibitor for mild steel in acidic environments.
- It contributes to the development of sustainable solutions for preventing corrosion in industrial applications.

Future research:

- Further studies are recommended to investigate the long-term performance and stability of CAE and similar inhibitors using computer-aided engineering tools.
- This will help refine these inhibitors and improve their effectiveness in real-world corrosion protection strategies.

References

1. M.M. Solomon, I.E. Uzoma, J.A.O. Olugbuyiro and O.T. Ademosun, A Censorious Appraisal of the Oil Well Acidizing Corrosion Inhibitors, *J. Pet. Sci. Eng.*, 2022, **215**, 110711. doi: [10.1016/j.petrol.2022.110711](https://doi.org/10.1016/j.petrol.2022.110711)
2. D. Wang, Y. Li, B. Chen and L. Zhang, Novel Surfactants as Green Corrosion Inhibitors for Mild Steel in 15% HCl: Experimental and Theoretical Studies, *Chem. Eng. J.*, 2020, **402**, 126219. doi: [10.1016/j.cej.2020.126219](https://doi.org/10.1016/j.cej.2020.126219)
3. B. El-Haitout, I. Selatnia, H. Lgaz, M.R. Al-Hadeethi, H.S. Lee, A. Chaouiki, Y.G. Ko, I.H. Ali and R. Salghi, Exploring the Feasibility of New Eco-Friendly Heterocyclic Compounds for Establishing Efficient Corrosion Protection for N80 Steel in a Simulated Oil Well Acidizing Environment: From Molecular-Level Prediction to Experimental Validation, *Colloids Surf., A*, 2023, **656**, 130372. doi: [10.1016/j.colsurfa.2022.130372](https://doi.org/10.1016/j.colsurfa.2022.130372)
4. B.D.B. Tiu and R.C. Advincula, Polymeric Corrosion Inhibitors for the Oil and Gas Industry: Design Principles and Mechanism, *React. Funct. Polym.*, 2015, **95**, 25–45. doi: [10.1016/j.reactfunctpolym.2015.08.006](https://doi.org/10.1016/j.reactfunctpolym.2015.08.006)

5. A.H. Alamri, Localized Corrosion and Mitigation Approach of Steel Materials Used in Oil and Gas Pipelines – An Overview, *Eng. Failure Anal.*, 2020, **116**, 104735. doi: [10.1016/j.engfailanal.2020.104735](https://doi.org/10.1016/j.engfailanal.2020.104735)
6. D.S. Chauhan, M.A.J. Mazumder, M.A. Quraishi and K.R. Ansari, Chitosan-cinnamaldehyde Schiff Base: A Bioinspired Macromolecule as Corrosion Inhibitor for Oil and Gas Industry, *Int. J. Biol. Macromol.*, 2020, **158**, 127–138. doi: [10.1016/j.ijbiomac.2020.04.200](https://doi.org/10.1016/j.ijbiomac.2020.04.200)
7. S. Şafak, B. Duran, A. Yurt and G. Türkoğlu, Schiff Bases as Corrosion Inhibitor for Aluminium in HCl Solution, *Corros. Sci.*, 2012, **54**, 251–259. doi: [10.1016/j.corsci.2011.09.026](https://doi.org/10.1016/j.corsci.2011.09.026)
8. F.E.T. Heakal and A.E. Elkholy, Gemini Surfactants as Corrosion Inhibitors for Carbon Steel, *J. Mol. Liq.*, 2017, **230**, 395–407. doi: [10.1016/j.molliq.2017.01.047](https://doi.org/10.1016/j.molliq.2017.01.047)
9. M. Farsak, H. Keleş and M.A. Keleş, New Corrosion Inhibitor for Protection of Low Carbon Steel in HCl Solution, *Corros. Sci.*, 2015, **98**, 223–232. doi: [10.1016/j.corsci.2015.05.036](https://doi.org/10.1016/j.corsci.2015.05.036)
10. R.G. Parr and R.G. Pearson, Absolute Hardness: Companion Parameter to Absolute Electronegativity, *J. Am. Chem. Soc.*, 1983, **105**, no. 26, 7512–7516. doi: [10.1021/ja00364a005](https://doi.org/10.1021/ja00364a005)
11. T.K. Chaitra, K.N.S. Mohana and H.C. Tandon, Thermodynamic, Electrochemical and Quantum Chemical Evaluation of Some Triazole Schiff Bases as Mild Steel Corrosion Inhibitors in Acid Media, *J. Mol. Liq.*, 2015, **211**, 1026–1038. doi: [10.1016/j.molliq.2015.08.031](https://doi.org/10.1016/j.molliq.2015.08.031)
12. R. Tambun, D.H. Sidabutar and V. Alexander, The potential of Petai peel as a zinc corrosion inhibitor in sodium chloride solution, *Int. J. Corros. Scale Inhib.*, 2020, **9**, no. 3, 929–940. doi: [10.17675/2305-6894-2020-9-3-8](https://doi.org/10.17675/2305-6894-2020-9-3-8)
13. J.N. Hasnidawani and H.N. Azlina, ZnO Nanoparticles for Anti-Corrosion Nanocoating of Carbon Steel, *Mater. Sci. Forum*, 2017, **894**, 76–80. doi: [10.4028/www.scientific.net/MSF.894.76](https://doi.org/10.4028/www.scientific.net/MSF.894.76)
14. S. Kouhi, B. Ghamari and R. Yeganeh, The Effect of NanoParticle Coating on Anticorrosion Performance of Centrifugal Pump Blades, *Jordan J. Mech. Ind. Eng.*, 2018, **12**, no. 2, 117–122.
15. S. Nath, S. Pityana and J.D. Majumdar, Laser surface alloying of aluminium with WC+Co+NiCr for improved wear resistance, *Surf. Coat. Technol.*, 2012, **206**, 3333–3341.
16. L.A. Khamaza, Generalized Diagram of the Ultimate Nominal Stresses (Endurance Limit) and the Corresponding Dimensions of the Non-Propagating Fatigue Cracks for Sharp and Blunt Notches, *Strength Mater.*, 2019, **51**, 350–360. doi: [10.1007/s11223-019-00081-w](https://doi.org/10.1007/s11223-019-00081-w)
17. Yu.G. Matvienko, Approaches of Fracture Mechanics in the Analysis of Admissible Defects in the Form of Notches, *Strength Mater.*, 2010, **42**, 58–63. doi: [10.1007/s11223-010-9188-2](https://doi.org/10.1007/s11223-010-9188-2)

18. D. Dwivedi, K. Lepková and T. Becker, Carbon steel corrosion: a review of key surface properties and characterization methods, *RSC Adv.*, 2017, **7**, 4580–4610. doi: [10.1039/C6RA25094G](https://doi.org/10.1039/C6RA25094G)
19. D.A. Winkler, Predicting the performance of organic corrosion inhibitors, *Metals*, 2017, **7**, no. 12, 553. doi: [10.3390/met7120553](https://doi.org/10.3390/met7120553)
20. C. Verma, L.O. Olasunkanmi, E.E. Ebenso and M.A. Quraishi, Substituents effect on corrosion inhibition performance of organic compounds in aggressive ionic solutions: a review, *J. Mol. Liq.*, 2018, **251**, 100–118. doi: [10.1016/j.molliq.2017.12.055](https://doi.org/10.1016/j.molliq.2017.12.055)
21. O. Kaczerewska, R. Leiva-Garcia, R. Akid, B. Brycki, I. Kowalczyk and T. Pospieszny, Heteroatoms and π electrons as favorable factors for efficient corrosion protection, *Mater. Corros.*, 2019, **70**, no. 6, 1099–1110. doi: [10.1002/maco.201810570](https://doi.org/10.1002/maco.201810570)
22. D.K. Verma, Y. Dewangan, A.K. Dewangan and A. Asatker, Heteroatom-Based Compounds as Sustainable Corrosion Inhibitors: An Overview, *J. Bio Tribo Corros.*, 2021, **7**, no. 15, 1–18. doi: [10.1007/s40735-020-00447-7](https://doi.org/10.1007/s40735-020-00447-7)
23. M. Athar, H. Ali and M.A. Quraishi, Corrosion inhibition of carbon steel in hydrochloric acid by organic compounds containing heteroatoms, *Br. Corros. J.*, 2002, **37**, no. 2, 155–158. doi: [10.1179/000705902225002376](https://doi.org/10.1179/000705902225002376)
24. S. Hadisaputra, A.A. Purwoko, I. Ilhamsyah, S. Hamdiani, D. Suhendra, N. Nuryono and B. Bundjali, A combined experimental and theoretical study of (*E*)-ethyl 3-(4-methoxyphenyl) acrylate as corrosion inhibitor of iron in 1 M HCl solutions, *Int. J. Corros. Scale Inhib.*, 2018, **7**, no. 4, 633–647. doi: [10.17675/2305-6894-2018-7-4-10](https://doi.org/10.17675/2305-6894-2018-7-4-10)
25. S. Hadisaputra, A.A. Purwoko, Rahmawati, D. Asnawati, Ilhamsyah, S. Hamdiani and Nuryono, Experimental and Theoretical Studies of (2R)-5-hydroxy-7-methoxy-2-phenyl-2,3-dihydrochromen-4-one as corrosion inhibitor for Iron in Hydrochloric Acid, *Int. J. Electrochem. Sci.*, 2019, **14**, no. 12, 11110–11121. doi: [10.20964/2019.12.77](https://doi.org/10.20964/2019.12.77)
26. A. Mohammed, H.S. Aljibori, M.A.I. Al-Hamid, W.K. Al-Azzawi, A.A.H. Kadhum and A. Alamiery, *N*-Phenyl-*N'*-[5-phenyl-1,2,4-thiadiazol-3-yl]thiourea: corrosion inhibition of mild steel in 1 M HCl, *Int. J. Corros. Scale Inhib.*, 2024, **13**, no. 1, 38–78. doi: [10.17675/2305-6894-2024-13-1-3](https://doi.org/10.17675/2305-6894-2024-13-1-3)
27. N.S. Abtan, A.E. Sultan, F.F. Sayyid, A.A. Alamiery, A.H. Jaaz, T.S. Gaaz, S.M. Ahmed, A.M. Mustafa, D.A. Ali and M.M. Hanoon, Enhancing corrosion resistance of mild steel in hydrochloric acid solution using 4-phenyl-1-(phenylsulfonyl)-3-thiosemicarbazide: A comprehensive study, *Int. J. Corros. Scale Inhib.*, 2024, **13**, no. 1, 435–459. doi: [10.17675/2305-6894-2024-13-1-22](https://doi.org/10.17675/2305-6894-2024-13-1-22)
28. J.A. Ibrahim, H.H. Ibraheem and H.T. Hussein, Experimental and theoretical studies on the corrosion inhibition potentials of *N'*-((1*H*-indole-3-yl)methylene)benzohydrazide for mild steel in HCl, *Int. J. Corros. Scale Inhib.*, 2024, **13**, no. 1, 94–120. doi: [10.17675/2305-6894-2024-13-1-6](https://doi.org/10.17675/2305-6894-2024-13-1-6)

-
29. A.N. Jasim, A. Mohammed, A.M. Mustafa, F.F. Sayyid, H.S. Aljibori, W.K. Al-Azzawi, A.A. Al-Amiery and E.A. Yousif, Corrosion Inhibition of Mild Steel in HCl Solution by 2-acetylpyrazine: Weight Loss and DFT Studies on Immersion Time and Temperature Effects, *Prog. Color, Color. Coat.*, 2024, **17**, no. 4, 333–350. doi: [10.30509/PCCC.2024.167231.1261](https://doi.org/10.30509/PCCC.2024.167231.1261)
 30. M.H. Abdulkareem, Z.A. Gbashi, B.A. Abdulhusein, M.M. Hanoon, A.A.H. Kadhum, A.A. Alamiery and W.K. Al-Azzawi, Investigating the corrosion inhibitory properties of 1-benzyl-4-imidazolidinone on mild steel in hydrochloric acid: a thorough experimental and quantum chemical study, *Int. J. Corros. Scale Inhib.*, 2024, **13**, no. 1, 411–434. doi: [10.17675/2305-6894-2024-13-1-21](https://doi.org/10.17675/2305-6894-2024-13-1-21)
 31. A.Y.I. Rubaye, M.T. Mohamed, M.A.I. Al-Hamid, A.M. Mustafa, F.F. Sayyid, M.M. Hanoon, A.H. Kadhum, A.A. Alamiery and W.K. Al-Azzawi, Evaluating the corrosion inhibition efficiency of 5-(4-pyridyl)-3-mercapto-1,2,4-triazole for mild steel in HCl: insights from weight loss measurements and DFT calculations, *Int. J. Corros. Scale Inhib.*, 2024, **13**, no. 1, 185–222. doi: [10.17675/2305-6894-2024-13-1-10](https://doi.org/10.17675/2305-6894-2024-13-1-10)
 32. N. Hamdi, A.S. Al-Ayed, R.B. Said and A. Fabienne, Synthesis and Characterization of New Thiazolidinones Containing Coumarin Moieties and Their Antibacterial and Antioxidant Activities, *Molecules*, 2012, **17**, no. 8, 9321–9334. doi: [10.3390/molecules17089321](https://doi.org/10.3390/molecules17089321)
 33. ASTM International, *Standard Practice for Preparing, Cleaning, and Evaluating Corrosion Test*, 2011, 1–9.
 34. S.S. Hadisaputra, A.A. Purwoko, A. Hakim, R. Wati, D. Asnawati and Y.P. Prananto, Experimental and Theoretical Study of Pinostrobin as Copper Corrosion Inhibitor at 1 M H₂SO₄ Medium, *IOP Conf. Ser.: Mater. Sci. Eng.*, 2020, **833**, no. 012010. doi: [10.1088/1757-899X/833/1/012010](https://doi.org/10.1088/1757-899X/833/1/012010)
 35. E.D. Akpan, A.K. Singh, H. Lgaz, T.W. Quadri, S.K. Shukla, B. Mangla, A. Dwivedi, O. Dagdag, E.E. Inyang and E.E. Ebenso, Coordination compounds as corrosion inhibitors of metals: A review, *Coord. Chem. Rev.*, 2024, **499**, 215503. doi: [10.1016/j.ccr.2023.215503](https://doi.org/10.1016/j.ccr.2023.215503)
 36. S. Hadisaputra, A.A. Purwoko, F. Wajdi, I. Sumarlan and S. Hamdiani, Theoretical study of the substituent effect on corrosion inhibition performance of benzimidazole and its derivatives, *Int. J. Corros. Scale Inhib.*, 2019, **8**, no. 3, 673–688. doi: [10.17675/2305-6894-2019-8-3-15](https://doi.org/10.17675/2305-6894-2019-8-3-15)
 37. NACE International, *Laboratory Corrosion Testing of Metals in Static Chemical Cleaning Solutions at Temperatures below 93°C (200°F)*, TM0193-2016-SG, 2000.
 38. A. Al-Amiery, Anti-Corrosion Performance Of 2-Isonicotinoyl-N-Phenylhydrazine-carbothioamide For Mild Steel Hydrochloric Acid Solution: Insights From Experimental Measurements And Quantum Chemical Calculations, *Surf. Rev. Lett.*, 2021, **28**, no. 3, 2050058. doi: [10.1142/S0218625X20500584](https://doi.org/10.1142/S0218625X20500584)

-
39. A.J.M. Eltmimi, A. Alamiery, A.J. Allami, R.M. Yusop, A.H. Kadhum and T. Allami, Inhibitive effects of a novel efficient Schiff base on mild steel in hydrochloric acid environment, *Int. J. Corros. Scale Inhib.*, 2021, **10**, no. 2, 634–648. doi: [10.17675/2305-6894-2021-10-2-10](https://doi.org/10.17675/2305-6894-2021-10-2-10)
40. A.A. Alamiery, Investigations on corrosion inhibitory effect of newly quinoline derivative on mild steel in HCl solution complemented with antibacterial studies, *Biointerface Res. Appl. Chem.*, 2022, **12**, no. 2, 1561–1568. doi: [10.33263/BRIAC122.15611568](https://doi.org/10.33263/BRIAC122.15611568)
41. V.C. Anadebe, V.I. Chukwuike, K.C. Nayak, E.E. Ebenso and R.C. Barik, Combined electrochemical, atomic scale-DFT and MD simulation of Nickel based metal organic framework (Ni-MOF) as corrosion inhibitor for X65 pipeline steel in CO₂-saturated brine, *Mater. Chem. Phys.*, 2024, **312**, 128606. doi: [10.1016/j.matchemphys.2023.128606](https://doi.org/10.1016/j.matchemphys.2023.128606)
42. A. Alamiery, W.N.R.W. Isahak, H. Aljibori, H. Al-Asadi and A. Kadhum, Effect of the structure, immersion time and temperature on the corrosion inhibition of 4-pyrrol-1-yl-N-(2,5-dimethyl-pyrrol-1-yl)benzoylamine in 1.0 M HCl solution, *Int. J. Corros. Scale Inhib.*, 2021, **10**, no. 2, 700–713. doi: [10.17675/2305-6894-2021-10-2-14](https://doi.org/10.17675/2305-6894-2021-10-2-14)
43. A. Alamiery, E. Mahmoudi and T. Allami, Corrosion inhibition of low-carbon steel in hydrochloric acid environment using a Schiff base derived from pyrrole: gravimetric and computational studies, *Int. J. Corros. Scale Inhib.*, 2021, **10**, no. 2, 749–765. doi: [10.17675/2305-6894-2021-10-2-17](https://doi.org/10.17675/2305-6894-2021-10-2-17)
44. M.J. Frisch, G.W. Trucks, H.B. Schlegel, G.E. Scuseria, M.A. Robb, J.R. Cheeseman, J.A. Montgomery, Jr., T. Vreven, K.N. Kudin, J.C. Burant, J.M. Millam, S.S. Iyengar, J. Tomasi, V. Barone, B. Mennucci, M. Cossi, G. Scalmani, N. Rega, G.A. Petersson, H. Nakatsuji, M. Hada, M. Ehara, K. Toyota, R. Fukuda, J. Hasegawa, M. Ishida, T. Nakajima, Y. Honda, O. Kitao, H. Nakai, M. Klene, X. Li, J.E. Knox, H.P. Hratchian, J.B. Cross, V. Bakken, C. Adamo, J. Jaramillo, R. Gomperts, R.E. Stratmann, O. Yazyev, A.J. Austin, R. Cammi, C. Pomelli, J.W. Ochterski, P.Y. Ayala, K. Morokuma, G.A. Voth, P. Salvador, J.J. Dannenberg, V.G. Zakrzewski, S. Dapprich, A.D. Daniels, M.C. Strain, O. Farkas, D.K. Malick, A.D. Rabuck, K. Raghavachari, J.B. Foresman, J.V. Ortiz, Q. Cui, A.G. Baboul, S. Clifford, J. Cioslowski, B.B. Stefanov, G. Liu, A. Liashenko, P. Piskorz, I. Komaromi, R.L. Martin, D.J. Fox, T. Keith, M.A. Al-Laham, C.Y. Peng, A. Nanayakkara, M. Challacombe, P.M.W. Gill, B. Johnson, W. Chen, M.W. Wong, C. Gonzalez and J.A. Pople, *Gaussian 03, Revision B. 05*, Gaussian, Inc., Wallingford, CT, 2004.
45. T. Koopmans, Ordering of wave functions and eigen-energies to the individual electrons of an atom, *Physica*, 1934, **1**, no. 1–6, 104–113 (in German). doi: [10.1016/S0031-8914\(34\)90011-2](https://doi.org/10.1016/S0031-8914(34)90011-2)
46. X. Wang, J. Liu, Z. Zhang, Q. Xiang, J. Zhang, L. Chen and H. Xie, Mechanism for corrosion inhibition of pure iron in 1 M HCl by *Rauvolfia Fujisana*: Experimental, GCMS, DFT, VASP and solidliquid modeling studies, *Ind. Crops Prod.*, 2024, **207**, 117692. doi: [10.1016/j.indcrop.2023.117692](https://doi.org/10.1016/j.indcrop.2023.117692)

-
47. A. Singh, A. Pandey, P. Banerjee, S. Saha, B. Chugh, S. Thakur, B. Pani, P. Chaubey and G. Singh, Eco-Friendly Disposal of Expired Anti-Tuberculosis Drug Isoniazid and Its Role in the Protection of Metal, *J. Environ. Chem. Eng.*, 2019, **7**, no. 2, 102971. doi: [10.1016/j.jece.2019.102971](https://doi.org/10.1016/j.jece.2019.102971)
48. M.S. Abdulazeez, Z.S. Abdullahe, M.A. Dawood, Z.K. Handel, R.I. Mahmood, S. Osamah, A.H. Kadhum, L.M. Shaker and A.A. Al-Amiery, Corrosion inhibition of low carbon steel in HCl medium using a thiadiazole derivative: weight loss, DFT studies and antibacterial studies, *Int. J. Corros. Scale Inhib.*, 2021, **10**, no. 4, 1812–1828. doi: [10.17675/2305-6894-2021-10-4-27](https://doi.org/10.17675/2305-6894-2021-10-4-27)
49. K. Cao, W. Li and L. Yu, Investigation of 1-Phenyl-3-Methyl-5-Pyrazolone as a corrosion inhibitor for mild steel in 1 M hydrochloric acid, *Int. J. Electrochem. Sci.*, 2012, **7**, 806–818.
50. A.Z. Salman, Q.A. Jawad, K.S. Ridah, L.M. Shaker and A.A. Al-Amiery, Selected BISThiadiazole: Synthesis and Corrosion Inhibition Studies on Mild Steel in HCl Environment, *Surf. Rev. Lett.*, 2020, **27**, no. 12, 2050014. doi: [10.1142/S0218625X20500146](https://doi.org/10.1142/S0218625X20500146)
51. A. Fouda, A. Al-Sarawy and E. El-Katori, Thiazole derivatives as corrosion inhibitors for C-steel in sulphuric acid solution, *Eur. J. Chem.*, 2010, **1**, no. 4, 312–318. doi: [10.5155/eurjchem.1.4.312-318.105](https://doi.org/10.5155/eurjchem.1.4.312-318.105)
52. M. Benabdellah, A. Tounsi, K. Khaled and B. Hammouti, Thermodynamic, Chemical and Electrochemical Investigations of 2-Mercapto Benzimidazole as Corrosion Inhibitor for Mild Steel in Hydrochloric Acid Solutions, *Arabian J. Chem.*, 2011, **4**, no. 1, 17–24. doi: [10.1016/j.arabjc.2010.06.010](https://doi.org/10.1016/j.arabjc.2010.06.010)
53. R. Haldhar, D. Prasad, A. Saxena and P. Singh, Valeriana Wallichii Root Extract as a Green & Sustainable Corrosion Inhibitor for Mild Steel in Acidic Environments: Experimental and Theoretical, *Mater. Chem. Front.*, 2018, **2**, no. 6, 1225–1237. doi: [10.1039/C8QM00120K](https://doi.org/10.1039/C8QM00120K)
54. A.K. Singh, S. Shukla and E. Ebenso, Cefacetrile as Corrosion Inhibitor for Mild Steel in Acidic Media, *Int. J. Electrochem. Sci.*, 2011, **6**, no. 11, 5689–5700. doi: [10.1016/S1452-3981\(23\)18437-9](https://doi.org/10.1016/S1452-3981(23)18437-9)
55. A. Alamiery, A. Mohamad, A. Kadhum and M. Takriff, Comparative data on corrosion protection of mild steel in HCl using two new thiazoles, *Data Brief*, 2022, **40**, 107838. doi: [10.1016/j.dib.2022.107838](https://doi.org/10.1016/j.dib.2022.107838)
56. Y. Zhang, Y. Cheng, F. Ma and K. Cao, Corrosion Inhibition of Carbon Steel by 1-Phenyl-3-Amino-5-Pyrazolone in H₂SO₄ solution, *Int. J. Electrochem. Sci.*, 2019, **14**, no. 1, 999–1008. doi: [10.20964/2019.01.69](https://doi.org/10.20964/2019.01.69)
57. A.S. Fouda, A.A. Al-Sarawy and E.E. El-Katori, Pyrazolone derivatives as corrosion inhibitors for C-steel in hydrochloric acid solution, *Desalination*, 2006, **201**, no. 1–3, 1–13. doi: [10.1016/j.desal.2006.03.519](https://doi.org/10.1016/j.desal.2006.03.519)

-
58. S. Hadisaputra, A.A. Purwoko, A. Hakim, L.R.T. Savalas, R. Rahmawati, S. Hamdiani and N. Nuryono, Ab *initio*MP2 and DFT studies of ethyl-p-methoxycinnamate and its derivatives as corrosion inhibitors of iron in acidic medium, *J. Phys.: Conf. Ser.*, 2019, **1402**, 055046. doi: [10.1088/1742-6596/1402/5/055046](https://doi.org/10.1088/1742-6596/1402/5/055046)
59. V.S. Sastri and J.R. Perumareddi, Molecular orbital theoretical studies of some organic corrosion inhibitors, *Corrosion*, 1997, **53**, no. 8, 617–622. doi: [10.5006/1.3290294](https://doi.org/10.5006/1.3290294)
60. Yu.I. Kuznetsov, N.N. Andreev and S.S. Vesely, Why we reject papers with calculations of inhibitor adsorption based on data on protective effects, *Int. J. Corros. Scale Inhib.*, 2015, **4**, no. 2, 108–109.
61. S. Hadisaputra, Z. Iskandar and D. Asnawati, Prediction of the Corrosion Inhibition Efficiency of Imidazole Derivatives: A Quantum Chemical Study, *Acta Chim. Asiana*, 2019, **2**, no. 1, 88–94. doi: [10.29303/aca.v2i1.15](https://doi.org/10.29303/aca.v2i1.15)
62. M. Gopiraman, N. Selvakumaran, D. Kesavan, I.S. Kim and R. Karvembu, Chemical and Physical Interactions of 1-Benzoyl-3,3-Disubstituted Thiourea Derivatives on Mild Steel Surface: Corrosion Inhibition in Acidic Media, *Ind. Eng. Chem. Res.*, 2012, **51**, no. 23, 7910–7922. doi: [10.1021/ie300048t](https://doi.org/10.1021/ie300048t)
63. A. Fouda and A. Hussein, Role of Some Phenylthiourea Derivatives as Corrosion Inhibitors for Carbon Steel in HCl Solution, *J. Korean Chem. Soc.*, 2012, **56**, no. 2, 264–273. doi: [10.5012/jkcs.2012.56.2.264](https://doi.org/10.5012/jkcs.2012.56.2.264)
64. A.S. Fouda, M.A. Ismail, A.S. Abousalem and G.Y. Elewady, Experimental and theoretical studies on corrosion inhibition of 4-amidinophenyl-2,2'-bifuran and its analogues in acidic media, *RSC Adv.*, 2017, **7**, 46414–46430. doi: [10.1039/C7RA08092A](https://doi.org/10.1039/C7RA08092A)
65. K.S. Bokati and C. Dehghanian, Adsorption behavior of 1*H*-benzotriazole corrosion inhibitor on aluminum alloy 1050, mild steel and copper in artificial seawater, *J. Environ. Chem. Eng.*, 2018, **6**, no. 2, 1613–1624. doi: [10.1016/j.jece.2018.02.015](https://doi.org/10.1016/j.jece.2018.02.015)
66. M. Mahdavian and S. Ashhari, Corrosion inhibition performance of 2-mercaptobenzimidazole and 2-mercaptobenzoxazole compounds for protection of mild steel in hydrochloric acid solution, *Electrochim. Acta*, 2010, **55**, no. 5, 1720–1724. doi: [10.1016/j.electacta.2009.10.055](https://doi.org/10.1016/j.electacta.2009.10.055)
67. S. Ahmadi and A. Khormali, Optimization of the corrosion inhibition performance of 2-mercaptobenzothiazole for carbon steel in HCl media using response surface methodology, *Fuel*, 2024, **357**, 129783. doi: [10.1016/j.fuel.2023.129783](https://doi.org/10.1016/j.fuel.2023.129783)
68. S.A. Abd El-Maksoud and A.S. Fouda, Some pyridine derivatives as corrosion inhibitors for carbon steel in acidic medium, *Mater. Chem. Phys.*, 2005, **93**, no. 1, 84–90. doi: [10.1016/j.matchemphys.2005.02.020](https://doi.org/10.1016/j.matchemphys.2005.02.020)
69. O. Krim, A. Elidrissi, B. Hammouti, A. Ouslim and M. Benkaddour, Synthesis, characterization, and comparative study of pyridine derivatives as corrosion inhibitors of mild steel in HCl medium, *Chem. Eng. Commun.*, 2009, **196**, no. 12, 1536–1546. doi: [10.1080/00986440903155451](https://doi.org/10.1080/00986440903155451)

-
70. K.R. Ansari, M.A. Quraishi and A. Singh, Pyridine derivatives as corrosion inhibitors for N80 steel in 15% HCl: Electrochemical, surface and quantum chemical studies, *Measurement*, 2015, **76**, 136–147. doi: [10.1016/j.measurement.2015.08.028](https://doi.org/10.1016/j.measurement.2015.08.028)
71. A.A.H. Kadhum, A.B. Mohamad, L.A. Hammed, A.A. Al-Amiery, N.H. San and A.Y. Musa, Inhibition of Mild Steel Corrosion in Hydrochloric Acid Solution by New Coumarin, *Materials*, 2014, **7**, no. 6, 4335–4348. doi: [10.3390/ma7064335](https://doi.org/10.3390/ma7064335)
72. M.M. Khowdiary, N.A. Taha, A.A. Barqawi, A.A. Elhenawy, M. Sheta and N. Hassan, Theoretical and experimental evaluation of the anticorrosion properties of new Coumarin's derivatives, *Alexandria Eng. J.*, 2022, **61**, no. 9, 6937–6948. doi: [10.1016/j.aej.2021.12.037](https://doi.org/10.1016/j.aej.2021.12.037)
73. A.A. Al-Amiery, Y.K. Al-Majedy, A.A. Kadhum and A.B. Mohamad, New coumarin derivative as an eco-friendly inhibitor of corrosion of mild steel in Acid medium, *Molecules*, 2014, **20**, no. 1, 366–383. doi: [10.3390/molecules20010366](https://doi.org/10.3390/molecules20010366)
74. D.K. Verma, S. Kaya, E. Ech-chihbi, F. El-Hajjaji, M.M. Phukan and H.M. Alnashiri, Investigations on some coumarin based corrosion inhibitors for mild steel in aqueous acidic medium: Electrochemical, surface morphological, density functional theory and Monte Carlo simulation approach, *J. Mol. Liq.*, 2021, **329**, 115531. doi: [10.1016/j.molliq.2021.115531](https://doi.org/10.1016/j.molliq.2021.115531)
75. A.M. Resen, M.M. Hanoon, W.K. Alani, A. Kadhim, A.A. Mohammed, T.S. Gaaz, A.A. Kadhum, A.A. Al-Amiery and M.S. Takriff, Exploration of 8-piperazine-1-ylmethylumbelliferone for application as a corrosion inhibitor for mild steel in hydrochloric acid solution, *Int. J. Corros. Scale Inhib.*, 2021, **10**, no. 1, 368–387. doi: [10.17675/2305-6894-2021-10-1-21](https://doi.org/10.17675/2305-6894-2021-10-1-21)
76. M.H. Yusoff, M.N. Azmi, M.H. Hussin, H. Osman, P.B. Raja, A.A. Rahim and K. Awang, An Electrochemical evaluation of synthesized coumarin-Azo dyes as potential corrosion inhibitors for mild steel in 1 M HCl medium, *Int. J. Electrochem. Sci.*, 2020, **15**, no. 12, 11742–11756. doi: [10.20964/2020.12.43](https://doi.org/10.20964/2020.12.43)
77. S.R. Krishnamurthy and M.H. Parameswaran, Synergistic effect of iodide ion and 4-hydroxy coumarin on the corrosion inhibition of mild steel in hydrochloric acid, *Int. Scholarly Res. Not.*, 2013, **2013**, 1–6. doi: [10.1155/2013/184787](https://doi.org/10.1155/2013/184787)
78. K.R. Ansari, M.A. Quraishi and A. Singh, Corrosion inhibition of mild steel in hydrochloric acid by some pyridine derivatives: an experimental and quantum chemical study, *J. Ind. Eng. Chem.*, 2015, **25**, 89–98. doi: [10.1016/j.jiec.2014.10.017](https://doi.org/10.1016/j.jiec.2014.10.017)
79. A.A. Farag, E.A. Mohamed, G.H. Sayed and K.E. Anwer, Experimental/computational assessments of API steel in 6 M H₂SO₄ medium containing novel pyridine derivatives as corrosion inhibitors, *J. Mol. Liq.*, 2021, **330**, 115705. doi: [10.1016/j.molliq.2021.115705](https://doi.org/10.1016/j.molliq.2021.115705)
80. A.A. Al-Amiery, W.N.R.W. Isahak and W.K. Al-Azzawi, Corrosion Inhibitors: Natural and Synthetic Organic Inhibitors, *Lubricants*, 2023, **11**, no. 4, 174. doi: [10.3390/lubricants11040174](https://doi.org/10.3390/lubricants11040174)

-
81. N.M. El Basiony, T. Tawfik, M.A. El-Raouf, A.A. Fadda and M.M. Waly, Synthesis, characterization, theoretical calculations (DFT and MC), and experimental of different substituted pyridine derivatives as corrosion mitigation for X-65 steel corrosion in 1 M HCl, *J. Mol. Struct.*, 2021, **1231**, 129999. doi: [10.1016/j.molstruc.2021.129999](https://doi.org/10.1016/j.molstruc.2021.129999)
82. A. Alrebh, M.B. Rammal and S. Omanovic, A pyridine derivative 2-(2-Methylaminoethyl)pyridine (MAEP) as a ‘green’ corrosion inhibitor for low-carbon steel in hydrochloric acid media, *J. Mol. Struct.*, 2021, **1238**, 130333. doi: [10.1016/j.molstruc.2021.130333](https://doi.org/10.1016/j.molstruc.2021.130333)
83. O. El Khattabi, B. Zerga, M. Sfaira, M. Taleb, M. Ebn Touhami, B. Hammouti, L. Herrag and M. Mcharfi, On the adsorption properties of an imidazole-pyridine derivative as corrosion inhibitor of mild steel in 1 M HCl, *Pharma Chem.*, 2021, **4**, no. 4, 1759–1768.
84. M.A. Dawood, Z.M.K. Alasady, M.S. Abdulazeez, D.S. Ahmed, G.M. Sulaiman, A.A.H. Kadhum, L.M. Shaker and A.A. Alamiery, The corrosion inhibition effect of a pyridine derivative for low carbon steel in 1 M HCl medium: Complemented with antibacterial studies, *Int. J. Corros. Scale Inhib.*, 2021, **10**, no. 4, 1766–1782. doi: [10.17675/2305-6894-2021-10-4-25](https://doi.org/10.17675/2305-6894-2021-10-4-25)
85. A. Ghazoui, R. Saddik, N. Benchat, M. Guenbour, B. Hammouti, S.S. Al-Deyab and A. Zarrouk, Comparative study of pyridine and pyrimidine derivatives as corrosion inhibitors of C38 steel in molar HCl, *Int. J. Electrochem. Sci.*, 2012, **7**, no. 8, 7080–7097. doi: [10.1016/S1452-3981\(23\)15769-5](https://doi.org/10.1016/S1452-3981(23)15769-5)
86. T.K. Chaitra, K.N. Mohana and H.C. Tandon, Study of new thiazole based pyridine derivatives as potential corrosion inhibitors for mild steel: theoretical and experimental approach, *Int. J. Corros.*, 2016, **2016**. doi: [10.1155/2016/9532809](https://doi.org/10.1155/2016/9532809)
87. A. Saady, Z. Rais, F. Benhiba, R. Salim, K.I. Alaoui, N. Arrousse, F. Elhajjaji, M. Taleb, K. Jarmoni, Y.K. Rodi, I. Warad and A. Zarrouk, Chemical, electrochemical, quantum, and surface analysis evaluation on the inhibition performance of novel imidazo[4,5-b] pyridine derivatives against mild steel corrosion, *Corros. Sci.*, 2021, **189**, 109621. doi: [10.1016/j.corsci.2021.109621](https://doi.org/10.1016/j.corsci.2021.109621)
88. A. Singh, K.R. Ansari, I.H. Ali, A.K. Alanazi, M. Younas and Y. Lin, Long chain imidazole derivative as a novel corrosion inhibitor for Q235 steel in 15% HCl medium under hydrodynamic condition: Experimental and theoretical examinations, *Mater. Chem. Phys.*, 2024, **313**, 128798. doi: [10.1016/j.matchemphys.2023.128798](https://doi.org/10.1016/j.matchemphys.2023.128798)
89. R.A. El-Nagar, N.A. Khalil, Y. Atef, M.I. Nessim and A. Ghanem, Evaluation of ionic liquids based imidazolium salts as an environmentally friendly corrosion inhibitors for carbon steel in HCl solutions, *Sci. Rep.*, 2024, **14**, no. 1, 1889. doi: [10.1038/s41598-024-52174-5](https://doi.org/10.1038/s41598-024-52174-5)

-
90. W. Ettahiri, M. Adardour, E. Ech-chihbi, M. Azam, R. Salim, S. Dalbouha, K. Min, Z. Rais, A. Baouid and M. Taleb, 1,2,3-triazolyl-linked benzimidazolone derivatives as new eco-friendly corrosion inhibitors for mild steel in 1 M HCl solution: Experimental and computational studies, *Colloids Surf., A*, 2024, **681**, 132727. doi: [10.1016/j.colsurfa.2023.132727](https://doi.org/10.1016/j.colsurfa.2023.132727)
91. N. Kedimar, P. Rao and S.A. Rao, Imidazole-based ionic liquid as a corrosion inhibitor for aluminum alloy and its composite in HCl – A comparative study, *Inorg. Chem. Commun.*, 2024, **160**, 112020. doi: [10.1016/j.inoche.2024.112020](https://doi.org/10.1016/j.inoche.2024.112020)
92. R.L. Camacho-Mendoza, E. Gutiérrez-Moreno, E. Guzmán-Percástegui, E. Aquino Torres, J. Cruz-Borbolla, J.A. Rodríguez-Ávila, J.G. Alvarado-Rodríguez, O. Olvera Neria, P. Thangarasu and J.L. Medina-Franco, Density functional theory and electrochemical studies: structure–efficiency relationship on corrosion inhibition, *J. Chem. Inf. Model.*, 2015, **55**, 2391–2402. doi: [10.1021/acs.jcim.5b00385](https://doi.org/10.1021/acs.jcim.5b00385)
93. K. Jrajri, F. Benhiba, M. Oubaaqa, S. Safi, A. Zaroual, M. El Moudane, I. Warad, D.R. Bazanov, N.A. Lozinskaya, A. Bellaouchou and A. Zarrouk, Electrochemical, surface and theoretical investigations of a new tri-tolyl imidazole designed for corrosion inhibition of carbon steel in normal hydrochloric acid medium, *Inorg. Chem. Commun.*, 2023, **157**, 111309. doi: [10.1016/j.inoche.2023.111309](https://doi.org/10.1016/j.inoche.2023.111309)
94. P. Wang, L. Fan, Y. Song, K. Deng, L. Guo, Z. Li and Y. Lin, Synergistic effect of new imidazoline derivative and 2-aminopyridine as corrosion inhibitors for Q235: Experimental and theoretical study, *Surf. Interface Anal.*, 2024, **56**, no. 4, 200–211. doi: [10.1002/sia.7286](https://doi.org/10.1002/sia.7286)

